On the importance of mechanisms analysis in the degradation of micropollutants by laccases: the case of Remazol Brilliant Blue R

Rosalie Pype[a,*], Sigrid Flahaut[b], Frédéric Debaste[a]

[a] *Department of Transfers, Interfaces and Processes, Université libre de Bruxelles, Av. F.D. Roosevelt 50, ULB CP165/67, 1050 Brussels, Belgium*
[b] *Department of Applied Microbiology, Université libre de Bruxelles c/o Labiris, Av. E. Gryson 1, 1070 Brussels, Belgium*

Abstract

The efficiency of methods to reduce the pollution induced by dyes is often evaluated using a color change measurement. This approach might hide complex mechanisms, that, if neglected, can lead to inadequate design of treatment units. This paper highlight this complexity on the case of Remazol Brilliant Blue R (RBBR), an industrial anthraquinone dye, degraded using *Trametes versicolor* laccases. A kinetic model describing the degradation of RBBR and the formation of degradation byproducts, one of which was found to have an orange color, is proposed. The complex links between RBBR degradation and the decolorization of the medium are highlighted, allowing to identify limits to the degradation achievable by the laccase in this case.

Keywords: Enzymatic degradation, Laccase, Model, Remazol Brilliant Blue R

1. Introduction

In recent years, pollution of surface and drinking waters by organic micropollutants has become a growing environmental issue. Micropollutants are substances which have a negative impact on organisms, even at very low concentrations (ng/L to μg/L). Their presence in the environment is often associated

*Corresponding author
Email addresses: rosapype@ulb.ac.be (Rosalie Pype), sflahaut@ulb.ac.be (Sigrid Flahaut), fdebaste@ulb.ac.be (Frédéric Debaste)

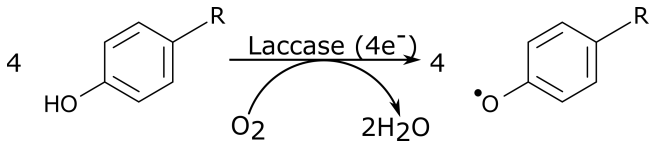

Figure 1: Action mechanism of laccases.

with negative impacts such as short and long term toxic effects, endocrine perturbation effects, antibiotics resistance development in microorganisms or, in the case of dyes, decrease of oxygen concentration in aquatic ecosystems due to the decrease of the amount of sunlight to photosynthetic organisms (Champagne and Ramsay, 2010; Fent et al., 2006; Pruden et al., 2006). Thus, the release of organic micropollutants in the environment should be avoided.

However, current wastewater treatment plants (WWTPs) are not specifically designed to remove micropollutants (Bolong et al., 2009; Luo et al., 2014; Petrović et al., 2003), especially because of the cost, the energy consumption and the non-specificity of presumably adequate treatments (ozonation, etc.). Therefore, numerous micropollutants are not sufficiently removed by WWTPs and end up in the natural environment at potentially problematic concentrations (Luo et al., 2014; Petrović et al., 2003).

A way to improve the organic micropollutants removal is the use of biodegradation processes such as enzymatic methods (Husain and Qayyum, 2013). Laccases are lignin-modifying enzymes found in white rote fungi (among other organisms) that show an interesting potential for the oxidation of highly recalcitrant organic micropollutants. Laccases can oxidize a broad range of molecules into radicals using molecular oxygen as an electron acceptor (Fig. 1). Their substrates include phenols, dyes, pesticides, endocrine disruptors and polycyclic aromatic hydrocarbons (Hautphenne et al., 2016; Majeau et al., 2010).

Remazol Brilliant Blue R (RBBR), an anthraquinone dye, is often used as a model-micropollutant to characterize laccases efficiency (see Table 1).

Occasionally, LC-MS is used as a way to identify degradation products but, often, RBBR degradation is only assessed by following the global decolorization

Table 1: Enzymatic degradation studies of RBBR: reasons of using RBBR and method of detection.

Use of RBBR	**Method of detection**	**References**
(One of several dyes used) to evaluate the decolorization of synthetic dyes	Spectrophotometer	(Champagne and Ramsay, 2010; Claus et al., 2002; Kunamneni et al., 2008)
Representative of an important class of recalcitrant anthraquinone-type dyes	Spectrophotometer, LC-MS[a]	(Hadibarata et al., 2011; Mechichi et al., 2006)
Representative of an important class of often toxic and recalcitrant organopollutants	Spectrophotometer, LC-MS[b]	(Deveci et al., 2004; Osma et al., 2010; Sathishkumar et al., 2013; Soares et al., 2001)
Indicator for detecting polychrorinated byphenil degradative activity	Spectrophotometer	(Nakagawa et al., 2010)

[a] used by (Hadibarata et al., 2011) to identify metabolites

[b] used by (Osma et al., 2010) to identify metabolites

of the medium at the wavelength of maximal absorbance of RBBR. This approach allows to assess the reduction of a precise problem in a less expensive way than more precise analytical methods. Yet, it does not give any information on the fate of the byproducts of the oxidation. Some of these byproducts could keep undesired side effects for the environment. Moreover, the global decolorization gives little insight into the kinetics of degradation, limiting the optimization and scale-up potential of this treatment method.

Thus, understanding the oxidation mechanism behind this decolorization is of interest. Some existing studies have tried to elucidate the decolorization mechanism qualitatively. Studying the decolorization of RBBR by free laccases of *Polyporus* sp. 133, Hadibarata et al. (2011) identified two degradation products as sodium 1-amino-9,10-dioxo-9,10-dihydroanthracene-2-sulfonate and sodium 2-((3-aminophenyl)sulfonyl)ethyl sulfate (see Fig. 2). The two same compounds were identified as reaction intermediates by Osma et al. (2010) using immobilized laccases of *Trametes pubescens*. They also identified two final byproducts (see Fig. 2) and proposed a degradation pathway on this basis.

Several studies determined the kinetic parameters of the laccase-catalyzed degradation of RBBR (see Table 2). These kinetic parameters were determined on the basis of spectrophotometric measurements. However, some degradation products could keep a residual absorbance and, then, using only a spectrophotometric approach could lead to a bad understanding of the kinetics. A better understanding of these kinetics would be helpful for the specific case of RBBR degradation but also in a more general framework to grasp the main type of mechanisms possibly involved in the degradation of organic micropollutants.

In this work, the relations between RBBR degradation, byproducts formation and global decolorization are studied in batch reactor using a spectrophotometer and, in some cases, a High Pressure Liquid Chromatograhy (HPLC) coupled to an UV detector. The experimental results are used to build and validate a kinetic model of the degradation, offering a deeper insight in the reaction mechanism.

Table 2: Kinetic parameters of the laccase-catalyzed degradation of RBBR (measurements by spectrophotometry).

Laccase-producing strain	**Laccase name**	**K_m (mM)**	**Reference**
Pleurotus ostreatus	POXA3	0.054	(Palmieri et al., 2005)
	POXC	0.051	
Pleurotus florida[a]		0.233	(Sathishkumar et al., 2013)
Aspergillus sp.[b,c]		0.064	(Soares et al., 2001)
Trametes pubescens		1.065	(Rodríguez-Couto, 2011)
Trametes hispida	Laccase I	3.5	(Rodríguez et al., 1999)
	Laccase II	3.9	

[a] Laccase-mediator system with 0.85 mM of *N*-hydroxybenzotriazole (HBT)

[b] Laccase produced by a genetically modified *Aspergillus* sp. strain

[c] Laccase purified from a commercial formulation provided by Novo Nordisk

2. Material and methods

2.1. Material

RBBR, laccase from *Trametes versicolor* presented as a powder with an activity of 12.9 U/mg, sodium azide, citric acid, $Na_2HPO_4.7H_2O$ and acetonitrile (ACN) of HPLC grade were purchased from Sigma Aldrich (Belgium). 2,2'-azino-bis(3-ethylbenzothiazoline-6-sulfonic acid) diammonium salt (ABTS) was purchased from VWR.

2.2. Methods

2.2.1. Laccase activity assays

Laccase activity was assessed by spectrophotometry using an ABTS assay as described in (Hautphenne and Debaste, 2015). A unit of activity is defined as the quantity of enzyme that degrade 1 μmol of ABTS per minute.

2.2.2. RBBR degradation

Degradations of RBBR were performed at pH 5 and 20°C (controlled temperature) in a magnetically stirred jacketed beaker using different enzymatic activities and different initial concentration of RBBR (see Table 3). The citrate-phosphate buffer was prepared as described in (Gomori, 1955). Laccases were dissolved into the buffer prior their adding to the reaction medium. Reaction time ranged from 1h to 4h depending on the assay. Samples were drawn at different reaction times, put in spectrophotometric cuvettes in which reaction was stopped by adding sodium azide to the medium (15 mM final concentration). Degradation assays were all monitored by spectrophotometry. Two assays (EXP8 and EXP9) were also monitored using HPLC-UV.

2.2.3. Spectrophotometer analyzes

The evolution of the absorbance of the reaction medium was measured with a spectrophotometer Hewlett Packard 8453 at wavelengths of 592 nm (wavelength of maximal absorbance for RBBR) and 475 nm (wavelength allowing to

Table 3: Experimental conditions used in the different assays. Temperature was controlled to be 20°C (maximum variability of 0.2°C); pH 5.0 (maximum variability of 0.2).

Assay	**$RBBR_0$ (mM)**		**E (U/L)**			**Reaction time (h)**
	th[1]	**exp**[2]	**th**[1]	**exp**[2]	**mod**[3]	
EXP1	0.03	0.0320	3500	[a]	2500	2
EXP2	0.30	0.305	3500	3000	3400	4
EXP3	0.30	0.307	3500	3400[b]	3400	4
EXP4	0.30	0.305	3500	3200	3200	2
EXP5	0.30	0.310	1000	900	1200	4
EXP6	0.30	0.310	2200	2200	2300	4
EXP7	0.30	0.315	3500	4200	3300	4
EXP8	1.00	1.17	3500	3000	2300	4
EXP9	1.00	1.20	3500	4200	3000	1

[1] Theoretical value

[2] Measured value

[3] Value giving the best fit between experimental data and model

[a] Enzymatic activity not measured

[b] Used for the adjustment of the parameters of the model

monitor the byproducts) at room temperature in 3mL-spectrophotometric cuvettes. The calibration curve for the RBBR concentration and its absorbance at 592 nm showed three distinct zones, each characterized by a specific linear relation between absorbance and concentration (see Fig. S.1 in Supporting Information).

The degree of decolorization (Y) is assessed by following the evolution of the absorbance associated with RBBR. This is calculated using:

$$\%Decolorization = Y = \frac{Abs_0 - Abs(t)}{Abs_0}$$

Where Abs_0 is the initial absorbance of the medium at 592 nm and $Abs(t)$ is the absorbance of the medium after a time t of reaction with laccase.

2.2.4. HPLC-UV analyzes

In two experiments (EXP8 and EXP9 in Table 3), evolutions of RBBR and its byproducts were monitored using a HPLC Waters e2695 with a detector Photodiode Waters 2998. The column used was an Ascentis RP-C18 column (250 x 4.6 mm, particule size 5 μm) (Sigma Aldrich) with the Empower Pro (version 6.1.2154.917) sofware. The column temperature was 30°C and the samples were maintained at 10°C. The injection volume was 20 μL and the flow-rate was 1 mL/min. The mobile phase was composed by solvent A: ACN and solvent B: milliQ water. The gradient elution program was: 0-10 min, 0-5% A; 10-25 min, 5-50% A; 25-40 min, 50-70% A and 40-50 min, 95% A. Samples were filtered (0.45 μm) before their injection in the HPLC.

RBBR degradation (X) is assessed by following the evolution of the area under the peak associated with RBBR and is calculated as follows:

$$\%Degradation = X = \frac{Area_0 - Area(t)}{Area_0}$$

Where $Area_0$ is the initial area under the RBBR peak and $Area(t)$ is the area under the RBBR peak after a time t of reaction with the laccase.

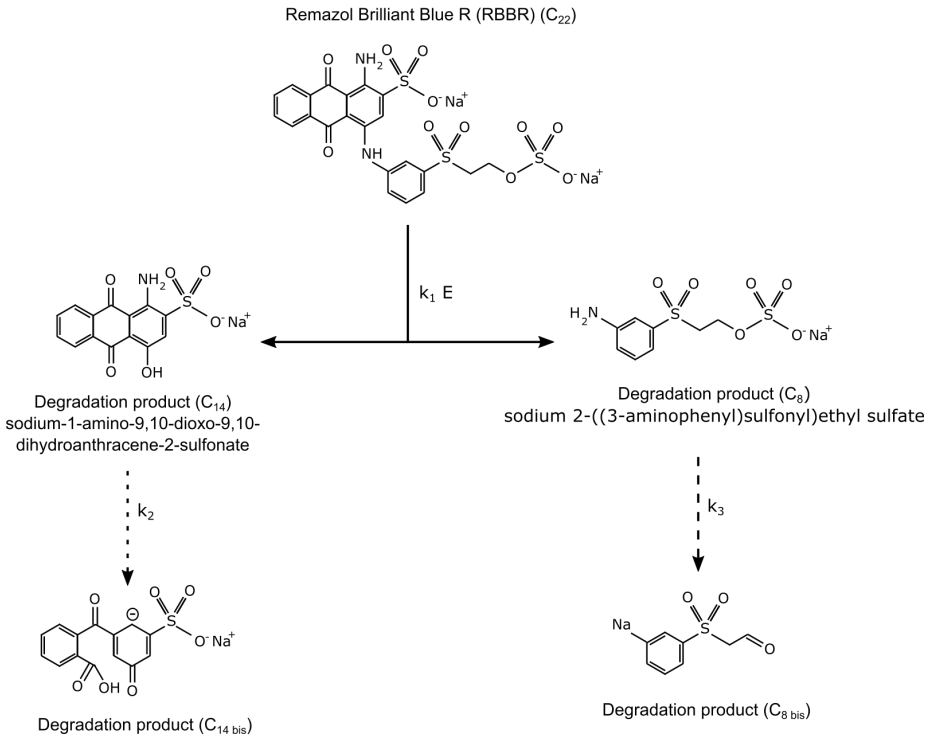

Figure 2: Considered degradation pathway of RBBR. Laccase splits RBBR in two parts forming the byproducts C_{14} and C_8 that can both be non-enzymatically transformed (based on (Hadibarata et al., 2011; Osma et al., 2010)).

2.2.5. Model development

According to the literature (Hadibarata et al., 2011; Osma et al., 2010), the laccase-catalyzed degradation pathway of RBBR seems to consist of a enzymatic cleavage of RBBR into two unstable byproducts that are further evolving by non-enzymatic reactions (Fig. 2). The 22 carbon atoms of the RBBR are split in two molecules containing respectively 14 and 8 carbons as the byproducts (C_{14} and C_8). During the further reactions, the number of carbons in the byproducts is considered stable.

This pathway can be modeled to evaluate the concentrations of RBBR (S_{22} (mol/L)) and its initial two byproducts (S_{14} and S_8 (mol/L)). The enzymatic reaction step could be modeled by Michaelis-Menten kinetics. However, a first

order kinetic was found to allow a good description of our data. So, for the sake of simplicity, a non-reversible first order kinetic law is used for this first step as well as for the further non enzymatic transformations. Mass balances on the different components in batch write:

$$\frac{dS_{22}}{dt} = -k_1\, E\, S_{22} \tag{1}$$

$$\frac{dS_{14}}{dt} = k_1\, E\, S_{22} - k_2\, S_{14} \tag{2}$$

$$\frac{dS_{8}}{dt} = k_1\, E\, S_{22} - k_3\, S_{8} \tag{3}$$

where t is the reaction time (s), E is the enzymatic activity (U/L), k_1 is the kinetic constant of the enzymatic degradation of RBBR (L/(U s)), k_2 and k_3 are the kinetic constants of the non-enzymatic degradation of C_{14} and C_8 (s^{-1}) respectively.

The solution of equations (1),(2),(3) with initial conditions $t = 0$, $S_{22} = RBBR_0$ and $S_{14} = S_8 = 0$ writes:

$$S_{22} = RBBR_0\, \exp\left(-k_1\, E\, t\right) \tag{4}$$

$$S_{14} = RBBR_0\, \frac{k_1\, E}{k_2 - k_1\, E} \left[\frac{S_{22}}{RBBR_0} - \exp\left(-k_2\, t\right)\right] \tag{5}$$

$$S_{8} = RBBR_0\, \frac{k_1\, E}{k_3 - k_1\, E} \left[\frac{S_{22}}{RBBR_0} - \exp\left(-k_3\, t\right)\right] \tag{6}$$

where $RBBR_0$ is the initial concentration of RBBR (mol/L).

Based on the comparison between the structure of the C_{14} byproduct and some anthraquinone dyes (see Fig. 3), C_{14} is supposed to absorb light in the range of the visible spectrum, leading to the observed shift of the color of the medium to a bright orange. Therefore, C_{14} could also present an absorbance at 592 nm (which is the wavelength of maximal absorbance for RBBR). In a similar way, RBBR absorbs light at 475 nm (see Fig. S.2 in Supplementary Information). The evolution of the absorbance of the medium at 592 nm and 475 nm can then be modeled by:

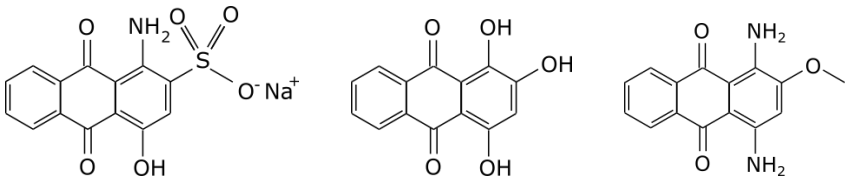

(a) C_{14} (b) Purpurin (c) Disperse red 11

Figure 3: Comparison of the structure of the C_{14} byproduct with those of some (red) anthraquinone dyes.

$$Abs_{592,mod} = \epsilon_{RBBR,592} \times l \times S_{22,mod} + \epsilon_{C_{14},592} \times l \times S_{14,mod} \quad (7)$$

$$Abs_{475,mod} = \epsilon_{RBBR,475} \times l \times S_{22,mod} + \epsilon_{C_{14},475} \times l \times S_{14,mod} \quad (8)$$

where Abs_{mod} is the modeled absorbance of the medium at 592 nm, $S_{22,mod}$ is the modeled concentration of RBBR (mol/L), $S_{14,mod}$ is the modeled concentration of the C_{14} byproduct (mol/L), l is the pathlength (1cm), $\epsilon_{RBBR,592}$ is the molar attenuation coefficient of RBBR at 592 nm (L mol^{-1} cm^{-1}), $\epsilon_{C_{14},592}$ is the molar attenuation coefficient of C_{14} at 592 nm (L mol^{-1} cm^{-1}), $\epsilon_{RBBR,475}$ is the molar attenuation coefficient of RBBR at 475 nm (L mol^{-1} cm^{-1}) and $\epsilon_{C_{14},475}$ is the molar attenuation coefficient of C_{14} at 475 nm (L mol^{-1} cm^{-1}).

The values of $\epsilon_{RBBR,592}$ and $\epsilon_{RBBR,475}$ were determined using calibration curves (see Fig. S.1 and S.2 in Supplementary Information).The values of k_1, k_2, $\epsilon_{C_{14},592}$ and $\epsilon_{C_{14},475}$ were determined by fitting the values predicted by (7) and (8) on the EXP3 data set using the least squares method. The values are summarized in Table 4.

As the C_8 byproduct was not detected during our experiments — because it does not absorb in the UV-Vis range — we were unable to determine the k_3 value. Therefore, the fate of C_8 will not be discussed any further.

Using equations (4), (5), (7) and (8), it is possible to evaluate the fastest possible color degradation. Indeed, with an infinite enzymatic activity, RBBR would be instantly transformed in C_{14} and C_8 which will then decay independently of the enzymatic activity. The lowest possible absorbance as a function

Table 4: Values of the parameters used in the model.

k_1 (L U^{-1} s^{-1})	k_2 (s^{-1})	$\epsilon_{C_{14},592}$ (L mol^{-1} cm^{-1})	$\epsilon_{C_{14},475}$ (L mol^{-1} cm^{-1})	$\epsilon_{RBBR,592}$ (L mol^{-1} cm^{-1})	$\epsilon_{RBBR,475}$ (L mol^{-1} cm^{-1})
$3.44\ 10^{-7}$	$1.33\ 10^{-5}$	567	1150	4678.8	727.1

of time writes:

$$Abs_{592,E\to\infty} = \epsilon_{C_{14},592} \times l \times RBBR_0 \exp(-k_2\, t) \quad (9)$$

$$Abs_{475,E\to\infty} = \epsilon_{C_{14},475} \times l \times RBBR_0 \exp(-k_2\, t) \quad (10)$$

3. Results and discussion

3.1. Evolution of the medium absorbance

Spectrophotometric data show that, at 592 nm, the absorbance of the medium decreases during the whole reaction. That decrease of absorbance is considerable during the first 40 minutes of the reaction and then much slower for the rest of the reaction (see Fig. 4 a and 6 a). The substantial decrease of the absorbance at 592 nm observed at the start of the reaction is mirrored by an increase of the absorbance at 475 nm (see Fig 4 b and 6 b). After reaching a maximum around 40 minutes of reaction, the absorbance at 475 nm slowly decrease during the rest of the reaction. These changes in the medium absorbance are directly observable as the color of the medium shift from blue to orange (see Fig. S.4 in Supporting Information).

3.2. Model validation

3.2.1. Direct validation

The determined values of the parameters are presented on Table 4. They were adjusted by fitting of the model on the EXP3 data set (see Fig. 4). The obtained value of the molar attenuation coefficient of C_{14} at 475 nm is higher than that obtained at 592 nm, which is coherent with the orange color that is supposed to be caused by C_{14}.

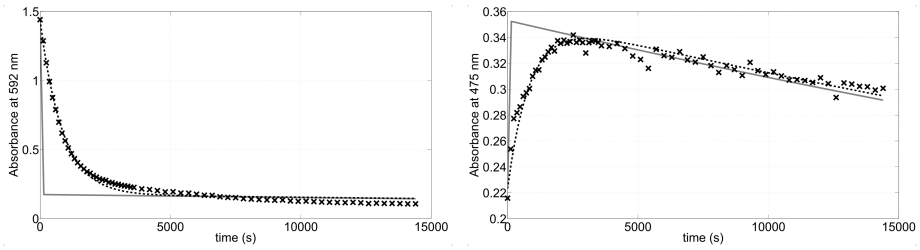

(a) Absorbance at 592 nm (b) Absorbance at 475 nm

Figure 4: Evolution of the absorbance of the medium during EXP3 (0.307 mM RBBR, E = 3400 U/L, 20°C, pH 5), '**x**' = measured data, doted line = EXP3 modeled data, gray plain line = modeled data for the limit case $E \to \infty$. The parameters values are presented in Table 4.

The model gives a good reproduction of the evolution of the measured data at both 592 nm and 475 nm (see Fig. 4).

The modeled data using an infinite enzymatic activity (plain gray line in Fig. 4) shows that past 2500 s the experimental remaining absorbance is at similar level to what would be achieved with infinite enzymatic activity. For this period, the experimental absorbance is dominated by the byproduct absorbance. Accelerating the enzymatic reaction, by rising the amount of enzyme in the system, will not allow to accelerate the absorbance reduction for these long times: in the proposed model, the enzyme has no impact on the degradation of C_{14}. The lack of ability of the enzyme to accelerate this step is a direct consequence of the proposed mechanism. Neglecting that mechanism and assuming that the color degradation is controlled only by the enzymatic reaction would not allow to get that conclusion.

3.2.2. Cross validation

The aim of this section is to test the ability of the model to predict absorbance values obtained for other data sets using the parameters values determined on EXP3 (see Table 4).

On a global point of view, the model gives the right trend of experimental data, for both wavelength (see Fig. 5). However, the values of the absorbance

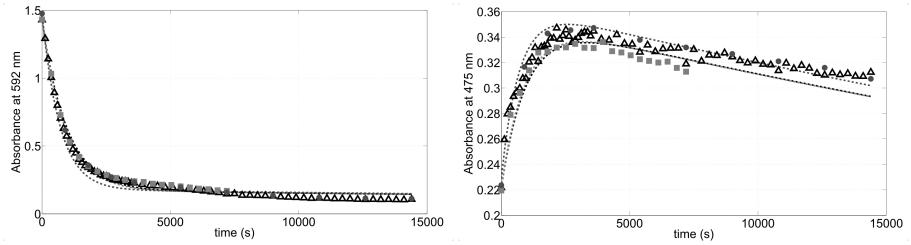

(a) Similar conditions of $RBBR_0$ and E than the data set used for adjustment

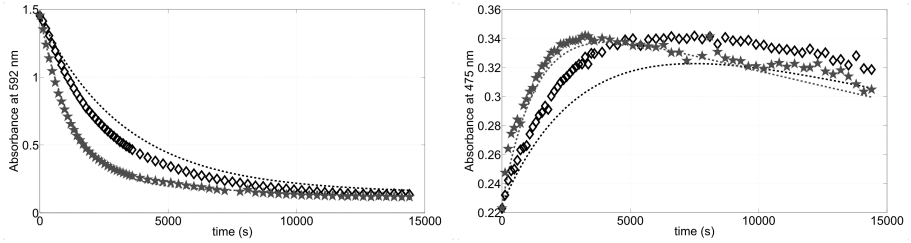

(b) Lower E

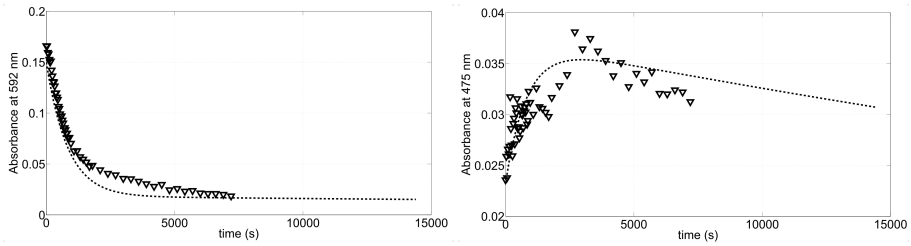

(c) Lower $RBBR_0$

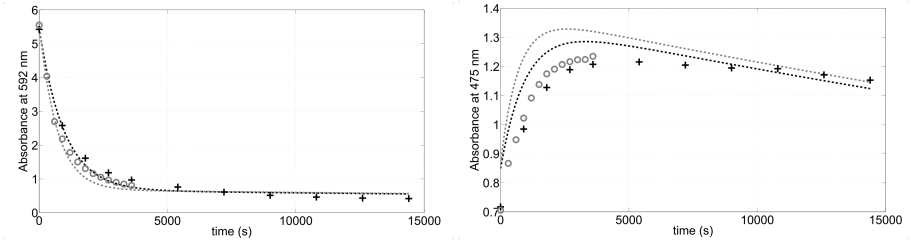

(d) Higher $RBBR_0$

Figure 5: Comparison of the model with other experimental data sets. The model appears as a doted line of the same color than the data set it describes. The modeled data were calculated using the measured values of E (see Table 3). The parameters values are presented in Table 4. All the experiments were realized at 20°C and pH5. (a) EXP2 = △ (0.305 mM RBBR, 3000 U/L), EXP4 = ■ (0.305 mM RBBR, 3200 U/L) and EXP7 = ● (0.315 mM RBBR, 4200 U/L), (b) EXP5 = ◊ (0.310 mM RBBR, 900 U/L) and EXP6 = ★ (0.310 mM RBBR, 2200 U/L), (c) EXP1 = ▽ (0.032 mM RBBR, 3500 U/L), (d) EXP8 = + (1.17 mM RBBR, 3000 U/L) and EXP9 = o (1.20 mM RBBR, 4200 U/L)

at 592 nm are (slightly) underestimated in the case of EXP1, EXP8 and EXP9 and overestimated in the case of EXP5. In a similar way, the values of the absorbance at 475 nm are overestimated in the case of EXP8 and EXP9 and underestimated in the case of EXP5. The values of modeled absorbance obtained for all the other experiments are really close to the measured values.

A better correspondence between measured and modeled data can be obtained by considering E to be slightly different of the measured E (see Table 3, graphs not shown). That highlight a possible imprecision on the measured E that reverberates on the modeled data.

The differences between the modeled and measured values appears principally in the case of experiments conducted using values of $RBBR_0$ or E quite distant of those of EXP3 (used for the parameters adjustment). The real mechanisms underlying the transformation can be more complex than those considered here. In particular in the case of the non-enzymatic transformation of C_{14} leading to differences between the modelled data and the measured data might be more complex than a single first order process. Also, only one byproduct (C_{14}) has been assumed to keep an absorbance. However, other compounds on the C_{14} reaction chain could have a residual absorbance as well. Despite those differences, it is clear that even with that simple model combining an enzymatic step and a non-enzymatic step, a good validation is obtained, showing the right trends.

3.3. HPLC analysis

HPLC analyses show one peak, Peak 1, at 592 nm before the start of the reaction. That peak corresponds to RBBR (see Table 5). Once the reaction started, a second peak, Peak 2, is detected at both 592 nm and 475 nm and three peaks, Peaks A, B and C, are detected at 475 nm (Fig. S.3 in Supplementary Information shows examples of the obtained HPLC spectra).

The comparison between the evolution of the medium absorbance monitored by spectrophotometry at 592 nm and the evolution of Peak 1 area shows that the observed decrease in the absorbance of the medium is caused by the degra-

Table 5: Characteristics of the peaks detected through HPLC analysis.

Peak name	**λ of detection**	**Retention time***	**Compound****
Peak 1	592 nm	20.3 – 22.9 min[a] 21.1 – 22.2 min[b]	RBBR
Peak 2	592 nm	29.4 – 29.9 min[a]	
	475 nm	28.6 – 28.9 min[b]	
Peak A	475 nm	20.8 – 21.6 min[a] 20.4 – 20.9 min[b]	C_{14}
Peak B	475 nm	22.4 – 23.4 min[a] 22.4 – 22.7 min[b]	
Peak C	475 nm	24.4 – 25.0 min[a] 23.7 – 24.1 min[b]	

* Retention times changed over time in relation with the concentrations

** Compound causing the peak when identified

[a] EXP8

[b] EXP9

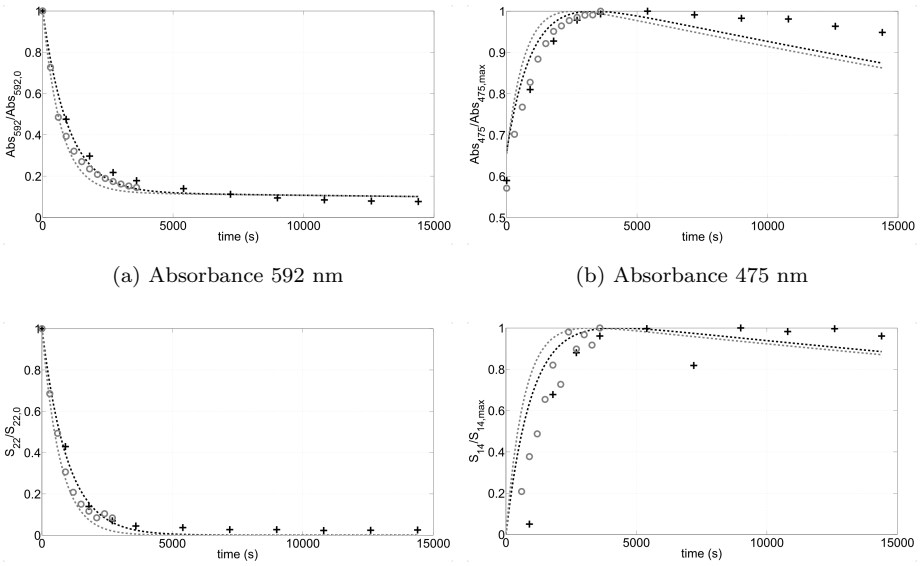

(a) Absorbance 592 nm

(b) Absorbance 475 nm

(c) Presence of RBBR

(d) Presence of C_{14}

Figure 6: RBBR degradation monitored by both spectrophotometry and HPLC-UV ($RBBR_0$ 1 mM, 20°C, pH 5). EXP8 = + and EXP9 = o, the model appears as a black doted line for EXP8 and as a gray plain line for EXP9. The parameters values are presented in Table 4. (a) Temporal evolution of the absorbance of the reactional medium at 592 nm (normalized by its initial value), (b) Temporal evolution of the absorbance of the reactional medium at 475 nm (normalized by its maximal value), (c) Temporal evolution of the area of Peak 1 detected at 592 nm by HPLC-UV (normalized by its initial value), (d) Temporal evolution of the area of Peak A detected at 475 nm by HPLC-UV (normalized by its maximal value).

dation of RBBR (Fig. 6 a and c). The higher absorbance retained with the spectrophotometry monitoring is caused by the residual absorbance of byproducts at 592 nm. Similarly, the comparison between the evolution of the medium absorbance monitored by spectrophotometry at 475 nm and the evolution of Peak A area shows that the observed increase in the absorbance of the medium is caused by the appearance of a byproduct (Fig. 6 b and d). On the basis of its absorbance capacity and the orange color than it gives to the medium, this byproduct is supposed to be C_{14} (Fig. 3). This suggests that C_{14} is formed relatively fast and is slowly degraded (Fig. 6 d).

The model gives a good prediction of the evolution of RBBR concentration even if values are slightly underestimated after the 5000 first seconds (see Fig. 6 (c)). The modeled values of C_{14} concentration follow the right trend (see Fig. 6 (d)).

Evolution of Peak B area is similar to that of Peak 1 (Fig. 7 a and Fig. 6 c), then Peak B is supposed to be caused by RBBR absorbing at 475 nm (maybe in an oxidized form). Evolutions of Peaks C and 2 are also similar as they present the same glitch for 40 and 45 min of reaction for EXP9 (Fig. 7 b and c). However, they cannot be caused by the same compound as they have really different retention times. So they are probably caused by two compounds whose fates are linked.

Comparison between decolorization results (obtained from evolution of the medium absorbance) and RBBR degradation results (obtained from the evolution of the peak area with HPLC-UV analysis) shows that using decolorization as an indicator of RBBR degradation leads to an underestimation of the real degradation (Fig. 8) of up to 10 %. It also shows that even a good RBBR degradation is not sufficient to make the medium colorless (see Fig. S.4 in Supporting Information). This can be explained by the fact that at least one of RBBR byproduct — identified as C_{14} on the basis of its structure — has an orange color.

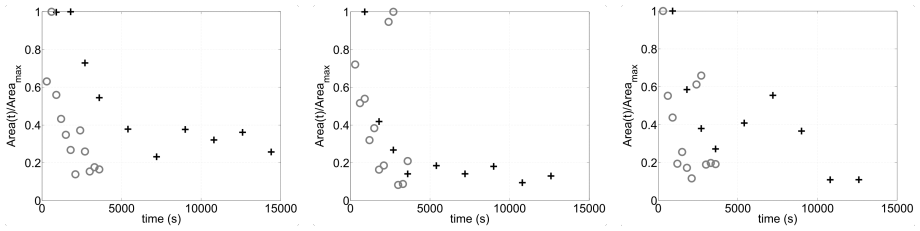

(a) Pic B (b) Pic C (c) Pic 2

Figure 7: Other results obtained for RBBR degradation monitored by HPLC-UV ($RBBR_0$ 1 mM, 20°C, pH 5), EXP8 = + and EXP9 = o, (a) Temporal evolution of the area of Peak B detected at 475 nm by HPLC-UV (normalized by its maximal value), (b) Temporal evolution of the area of Peak C detected at 475 nm by HPLC-UV (normalized by its maximal value), (c) Temporal evolution of the area of Peak 2 detected at 592 nm by HPLC-UV (normalized by its maximal value).

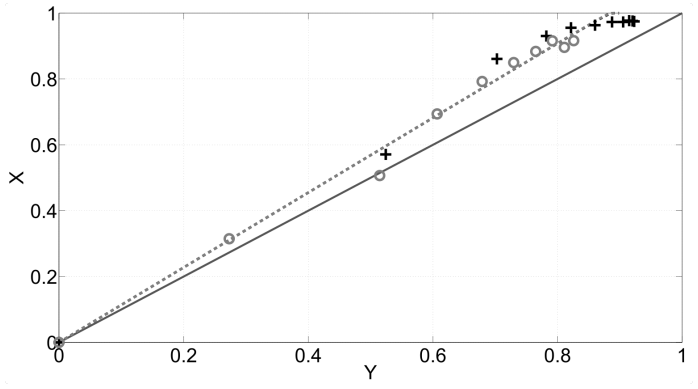

Figure 8: Comparison between decolorization of the medium (Y) and RBBR degradation (X). EXP8 = + and EXP9 = o, plain line = Y=X. The modeled data of the two experiments overlap in this case.

4. Conclusion

During the enzymatic degradation of RBBR, a significant difference (up to 10 %) appears between the level of RBBR degradation and the level of obtained decolorization. The estimation of RBBR degradation based only on the degree of decolorization of the medium is underestimated. This can be attributed to the existence of a reaction mechanism in which some by-product still absorb in the visible range. Using only the decolorization as factor to evaluate the kinetics and to design treatment solutions could lead to wrong evaluation of the amount of enzymes to use. This stresses the importance of understanding the mechanisms underlying the reaction when dealing with micropollutants degradation.

Yet, the model proposed here to describe the degradation of RBBR and the formation of degradation products stays quite simple but is able to have a significant predictive ability. Contrary to a single first order equation, the developed model allows to take into account the existence of a maximum degradation achievable in a given time using laccases, even with a very large amount of enzymes. That observation is important in the objective to develop a laccase-based treatment of RBBR and other dyes that could present similar behavior when reacting with laccases.

Declaration of interest

Declarations of interest: none

Acknowledgments

Rosalie Pype acknowledges financial support from the Fonds pour la Formation à la Recherche dans l'Industrie et dans l'Agriculture (FRIA), Brussels, Belgium.

References

Bolong, N., Ismail, A. F., Salim, M. R., Matsuura, T., Apr. 2009. A review of the effects of emerging contaminants in wastewater and options for their removal. Desalination 239 (1-3), 229–246.

Champagne, P.-P., Ramsay, J. A., Apr. 2010. Dye decolorization and detoxification by laccase immobilized on porous glass beads. Bioresour. Technol. 101 (7), 2230–2235.

Claus, H., Faber, G., König, H., Sep. 2002. Redox-mediated decolorization of synthetic dyes by fungal laccases. Appl. Microbiol. Biotechnol. 59 (6), 672–678.

Deveci, T., Unyayar, A., Mazmanci, M. A., Jul. 2004. Production of Remazol Brilliant Blue R decolourising oxygenase from the culture filtrate of Funalia trogii ATCC 200800. J. Mol. Catal. B: Enzym. 30 (1), 25–32.

Fent, K., Weston, A., Caminada, D., Feb. 2006. Ecotoxicology of human pharmaceuticals. Aquat. Toxicol. 76 (2), 122–159.

Gomori, G., 1955. Preparation of buffers for use in enzyme studies. In: Methods in Enzymology. Vol. 1. Elsevier, pp. 138–146.

Hadibarata, T., Yusoff, A. R. M. M., Kristanti, R. A., Aug. 2011. Decolorization and Metabolism of Anthraquionone-Type Dye by Laccase of White-Rot Fungi Polyporus sp. S133. Water, Air, Soil Pollut. 223 (2), 933–941.

Hautphenne, C., Debaste, F., Jul. 2015. Harnessing Laccases for the Synthesis of Bisphenol A Biopolymers. Chem. Eng. Technol. 38 (7), 1223–1228.

Hautphenne, C., Penninckx, M., Debaste, F., Apr. 2016. Product formation from phenolic compounds removal by laccases: A review. Environ. Technol. Innovat. 5, 250–266.

Husain, Q., Qayyum, S., Sep. 2013. Biological and enzymatic treatment of bisphenol A and other endocrine disrupting compounds: a review. Crit. Rev. Biotechnol. 33 (3), 260–292.

Kunamneni, A., Ghazi, I., Camarero, S., Ballesteros, A., Plou, F. J., Alcalde, M., Feb. 2008. Decolorization of synthetic dyes by laccase immobilized on epoxy-activated carriers. Process Biochem. 43 (2), 169–178.

Luo, Y., Guo, W., Ngo, H. H., Nghiem, L. D., Hai, F. I., Zhang, J., Liang, S., Wang, X., Mar. 2014. A review on the occurrence of micropollutants in the aquatic environment and their fate and removal during wastewater treatment. Sci.Total Environ. 473-474, 619–641.

Majeau, J. A., Brar, S. K., Tyagi, R. D., Apr. 2010. Laccases for removal of recalcitrant and emerging pollutants. Bioresour. Technol. 101 (7), 2331–2350.

Mechichi, T., Mhiri, N., Sayadi, S., Aug. 2006. Remazol Brilliant Blue R decolourization by the laccase from Trametes trogii. Chemosphere 64 (6), 998–1005.

Nakagawa, Y., Sakamoto, Y., Kikuchi, S., Sato, T., Yano, A., Jul. 2010. A chimeric laccase with hybrid properties of the parental lentinula edodes laccases. Microbiol. Res. 165 (5), 392–401.

Osma, J. F., Toca-Herrera, J. L., Rodríguez-Couto, S., Nov. 2010. Transformation pathway of Remazol Brilliant Blue R by immobilised laccase. Bioresour. Technol. 101 (22), 8509–8514.

Palmieri, G., Cennamo, G., Sannia, G., Jan. 2005. Remazol Brilliant Blue R decolourisation by the fungus Pleurotus ostreatus and its oxidative enzymatic system. Enzyme Microb. Technol. 36 (1), 17–24.

Petrović, M., Gonzalez, S., Barceló, D., Nov. 2003. Analysis and removal of emerging contaminants in wastewater and drinking water. TrAC, Trends Anal. Chem. 22 (10), 685–696.

Pruden, A., Pei, R., Storteboom, H., Carlson, K. H., Dec. 2006. Antibiotic Resistance Genes as Emerging Contaminants: Studies in Northern Colorado. Environ. Sci. Technol. 40 (23), 7445–7450.

Rodríguez, E., Pickard, M. A., Vazquez-Duhalt, R., Jan. 1999. Industrial dye decolorization by laccases from ligninolytic fungi. Curr. Microbiol. 38 (1), 27–32.

Rodríguez-Couto, S., Oct. 2011. Production of laccase and decolouration of the textile dye Remazol Brilliant Blue R in temporary immersion bioreactors. J. Hazard. Mater. 194, 297–302.

Sathishkumar, P., Balan, K., Palvannan, T., Kamala-Kannan, S., Oh, B. T., Rodríguez-Couto, S., Jul. 2013. Efficiency of Pleurotus florida Laccase on Decolorization and Detoxification of the Reactive Dye Remazol Brilliant Blue R (RBBR) under Optimized Conditions. CLEAN 41 (7), 665–672.

Soares, G. M. B., de Amorim, M. T. P., Costa-Ferreira, M., Aug. 2001. Use of laccase together with redox mediators to decolourize Remazol Brilliant Blue R. J. Biotechnol. 89 (2–3), 123–129.

Supporting Information

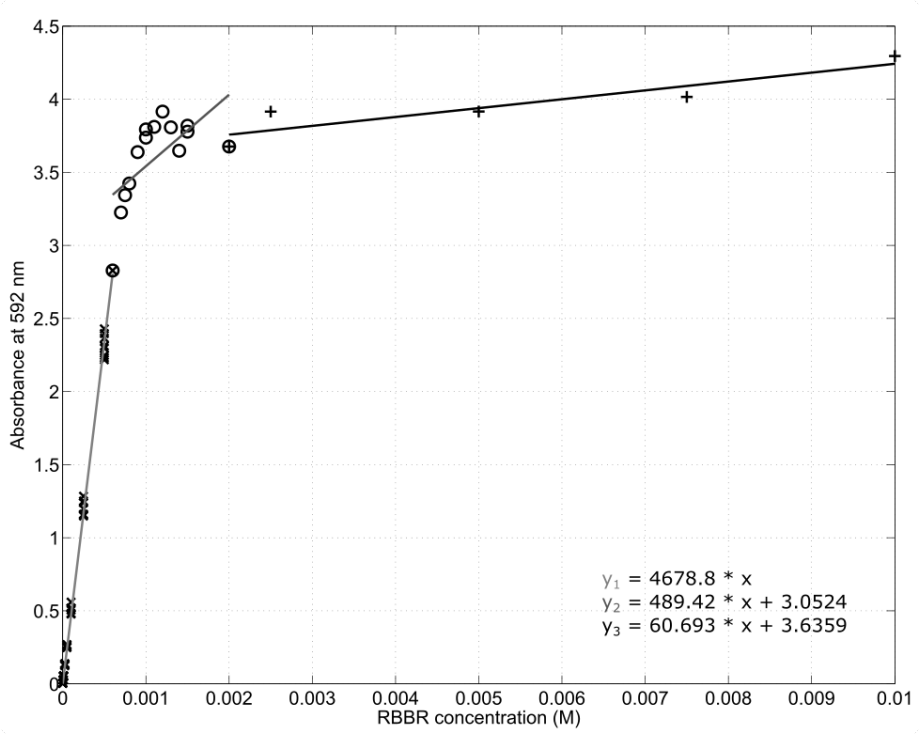

Figure S.1: Calibration curves with correspondence between absorbance at 592 nm and RBBR concentration. Three zones of correspondence are present, each with its own linear relation between absorption and RBBR concentration. The first zone corresponds to the linearity zone and describes correspondence for concentration ranging from 0 to 0.6 mM ('**x**' = experimental data, '—' = linear relation: $y_1 = 4678.8 \times x$). The second zone describes correspondence for concentration ranging from 0.6 to 2 mM ('**o**' = experimental data, '—' = linear relation: $y_2 = 489.42 \times x + 3.0524$). The third zone describes correspondence for concentration above 2 mM ('**+**' = experimental data, '—' = linear relation: $y_3 = 60.693 \times x + 3.6359$).

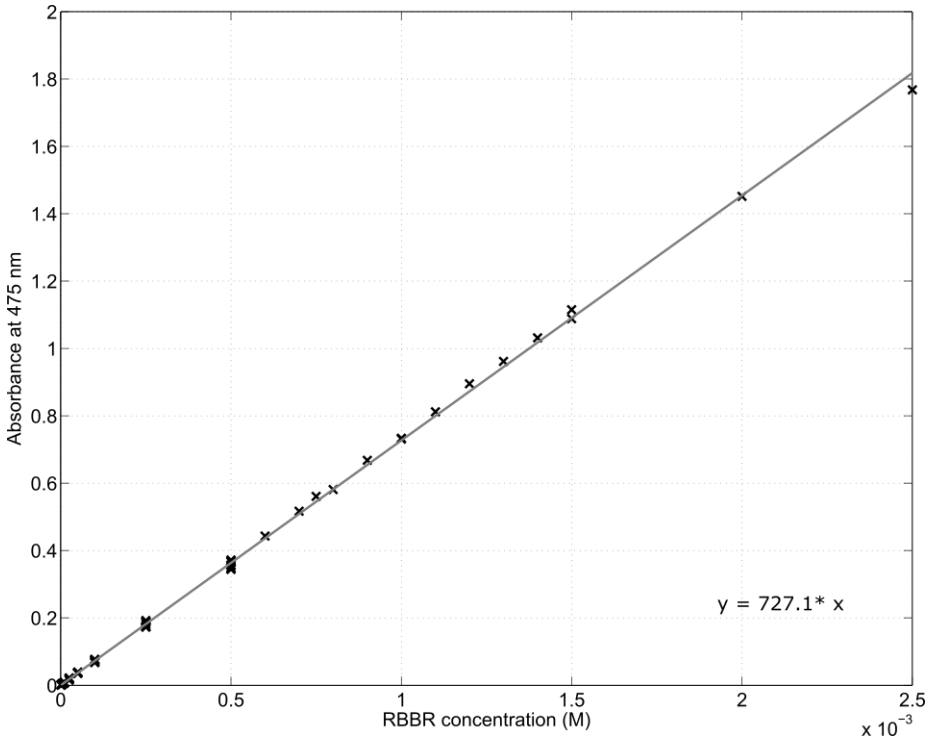

Figure S.2: Calibration curve with correspondence between absorbance at 475 nm and RBBR concentrations. The linear relation between absorption at 475 nm and RBBR concentration is described by: $y = 727.1 \times x$. '**x**' = experimental data, '—' = linear relation

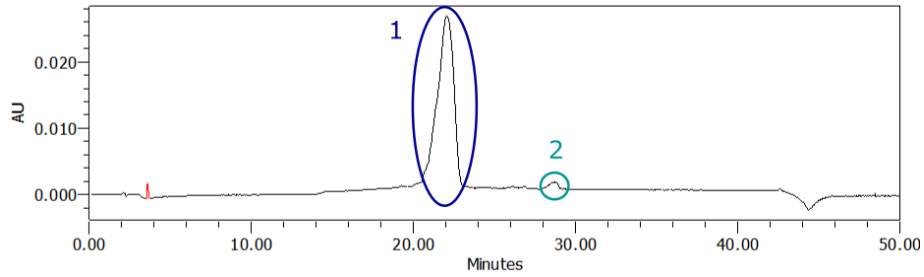

(a) 592 nm

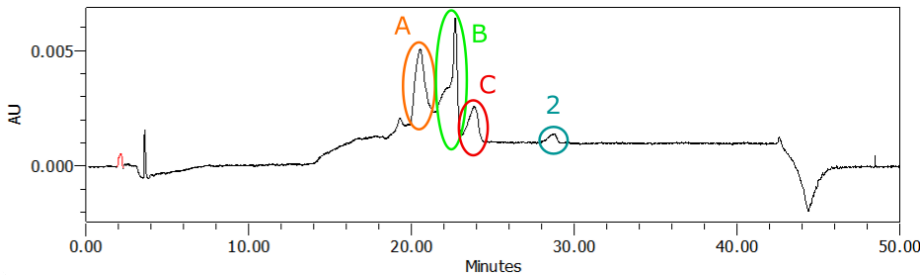

(b) 475 nm

Figure S.3: HPLC spectra obtained for the analysis of the reaction medium of EXP9 after 15 minutes of reaction. The different peaks are labeled on the spectra.

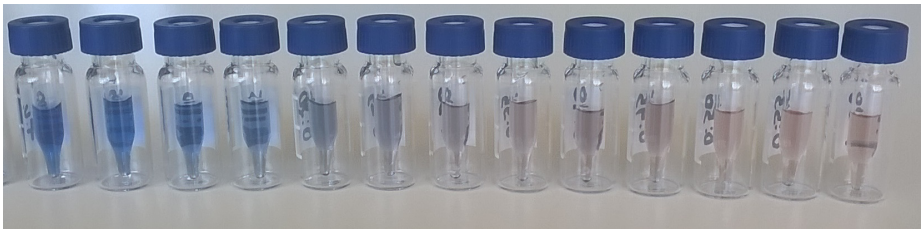

Figure S.4: Color change through enzymatic reaction of 1.20 mM RBBR and 4200 U/L laccases. Left: start of the reaction (0h) to right: 1h of reaction. Samples were withdrawn every 5 minutes and laccases were deactivated using sodium azide.